ISSN 1392-1320 MATERIALS SCIENCE (MEDŽIAGOTYRA). Vol. XX, No. X. 2027

Phase Evolution and Cu Partitioning of Amorphous $Ti_{30}Cu_{70}$ Ribbons in Liquid Sn at 590 °C

Zijie WANG [1], Jingyi ZHOU [1], Chengyuan TAO [1], Peng ZHANG [2], Zhenhua DAN [1] *

[1] *College of Materials Science and Engineering, Nanjing Tech University, Nanjing 211816, China*
[2] *Jiangsu Tiangong Technology Co., Ltd., Zhenjiang 212413, China*

http://doi.org/10.5755/j02.ms.44678

Received 31 March 2026; accepted 18 June 2026

Elemental redistribution is able to achieve through thermal diffusion and formation of intermetallic phases in amorphous $Ti_{30}Cu_{70}$ ribbons in liquid Sn at 590 °C. Cu elements are replaced partially by Sn elements gradually with the extension of treatment time, and most of Cu elements can be replaced by Sn at 60 s. Preformed Ti_2Cu intermetallic phases in amorphous $Ti_{30}Cu_{70}$ ribbons still remain as preformed due to their higher thermal stability than Sn-containing intermetallics. Both Ti_6Sn_5 and Ti_2Sn_3 intermetallic phases are preferred to form after thermal diffusion for 60 s. The repartitioning rate of Sn elements is confirmed to be 5.61×10^{-8} m s^{-1} according to the change of the thickness of residual layers with high Cu concentration. The present methodology provides a possible alloying way to fabricate the precursors with multilayers where different intermetallic phases are distributed.

Keywords: thermal diffusion, elemental repartitioning, intermetallic phase, chemical etching.

1. INTRODUCTION

Sn with a low melting temperature of 232 °C [1], is widely used in low-temperature soldering processes. The smelting Sn pool can be used to build up a liquid-solid reaction environment for fast elemental diffusion. The diffusion coefficient of Cu in molten Sn is several orders of magnitude greater than that in solid Sn, and more favorable formations for variohe us intermetallic compounds are ascribed to the solid-liquid diffusion [2]. The localized diffusion of Sn into Cu foams can drive the formation of various intermetallic phases (IMCs) with different morphology, including Cu_6Sn_5 IMC with a melting point of 227 °C and porous Cu_3Sn IMC with melting point of 415 °C [3 – 5]. These physicochemical reactions are sensitive to the temperature and related to the thermal stability of the newly formed intermetallic phases. Above-mentioned works give us a hint that the proper reaction time and temperature are able to trigger the thermal diffusion of Sn into other metallic matrix and make accurate tailoring of the intermetallic distribution, both thickness and chemical composition of the intermetallic layers [6, 7].

Amorphous alloys are composed of uniformly distributed alloying elements and are absent of grain boundaries and intermetallic phases [8]. Uniformity in chemical composition and microstructure is good for the uniform invasion of highly active elements via thermal diffusion. As reported before, binary Ti-Cu amorphous alloys have been fabricated by the using melt spinning method and the amorphous ribbons are formed after rapid quenching solidification [9]. However, partially crystallized $Ti_{30}Cu_{70}$ ribbons are reported to consist of amorphous matrix and Ti_2Cu_3 IMC. In our previous work, thermal diffusion has been employed to fabricate layered distributed AlCu IMCs with a gradient chemical composition in Al/Cu stacking foils [10]. Different Al_2Cu and Cu_3Al IMCs form at different regions with a layered structure through the interdiffusion and IMC formation [10]. The relativly slower solid-solid interdiffusion in the solid states restricts the fast movements of the diffusion tips and the formation of the IMCs. Replacement of the alloying elements can take place when the interdiffusion process proceeds fast enough, as previously reported [3, 9, 10].

Thermal diffusion between liquid Sn and solid Cu foams and layered IMC formation provide us a new strategy to motivate the redistribution of alloying elements. Fast thermal diffusion of alloying elements in liquid Sn at higher temperatures can replace alloying elements by diffused Sn atoms and form the new IMCs. The directional and concentration gradient governed diffusion helps to form multipayer microstructure, which causes heterogeneity in the chemical composition and structure simultaneously. $Ti_{30}Cu_{70}$ alloy with minor Ti_2Cu IMC is selected to investigate repartitioning behavior of Cu and Ti and the effect of thermal stability of IMCs on the microstructural evolution. The present research aims to establish a methodology for designing and fabricating of expected alloys or precursors with controllable layered microstructure and predictable chemical composition based on the elemental redistribution during thermal alloying in liquid metals.

2. EXPERIMENTAL PROCEDURE

Binary Ti-Cu alloys with nominal compositions of 70 at.% Cu were prepared by arc melting of the mixture of pure Ti (99.99 wt.%) and pure Cu (99.9 wt.%) in an Ar atmosphere. The melt spinning method, detailed previously [11], was used to prepare $Ti_{30}Cu_{70}$ amorphous ribbons with

* Corresponding author: Z. Dan
E-mail: *zhenhuadan@njtech.edu.cn*

a thickness of 40.3 μm and 2 mm in width. The experimental procedures are shown in Fig. 1.

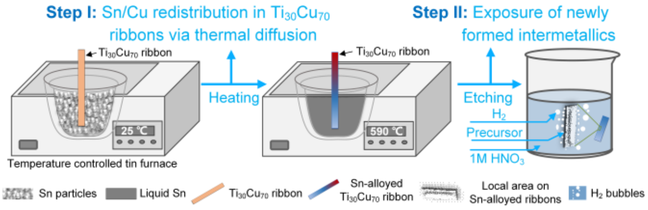

Fig. 1. Schematics of experimental process including thermal diffusion and chemical etching for exposure the newly-formed intermetallic phases in $Ti_{30}Cu_{70}$ amorphous ribbons

In Step I, as-spun ribbons were inserted into Sn smelts (99.99 wt.%) in the temperature controlled tin furnace. Thermal diffusion was conducted at 590 °C for 5, 30 and 60 s. In order to charaterize the morphology of newly formed intermetallics, chemical ething was conducted in 1 M HNO_3 solution for 18 h in Step II. The diffusion kinetics of Sn elements and Cu repartitioning are reflected by the invasion depth of Sn and the thickness of the residual TiCu layer via the cross-sectional SEM observation (SEM, ZEISS, Sigma 300) equipped with an energy dispersive X-ray spectroscope. The phase composition of as-spun and ecthed samples was characterized by an X-ray diffractometer (XRD, Rigaku, Geigerflex) with a radiation source of Cu Kα (λ = 0.154 nm).

3. RESULTS AND DISCUSSION

3.1. Initial microstructural characteristics of as-spun amorphous $Ti_{30}Cu_{70}$ ribbons

XRD pattern of as-spun $Ti_{30}Cu_{70}$ ribbons in Fig. 2 a consists of a single wide peak centered at 43.3°, indicating the ribbon is in an amorphous state.

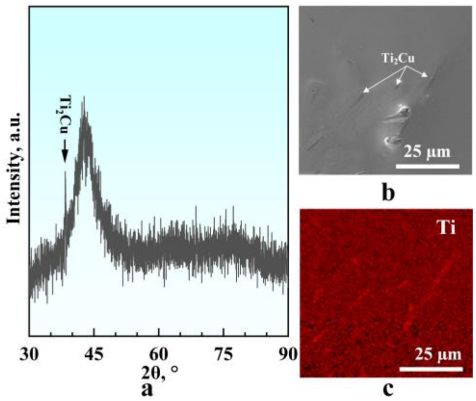

Fig. 2. As-spun $Ti_{30}Cu_{70}$ amorphous ribbons: a – XRD pattern; b – surface morphology; c – Ti elemental mapping

Besides the main diffusion peak, the sharp peak centered at 38.36° is assigned to Ti_2Cu phase (JCPDF Card No.:15-0717). The contrast difference in different regions in Fig. 2 b demonstrates difference in Ti concentration, which is consistent with Ti elemental mapping in Fig. 2 c. The Ti-to-Cu ratios in different regions are confirmed close to 3:7 and 7:3 by EDS in Table 1. Thus, many bar-shaped crystalline Ti_2Cu precipitates randomly distribute inside the amorphous matrix. Amorphous matrix and randomly distributed Ti_2Cu intermetallic in $Ti_{30}Cu_{70}$ alloy are considered to have different thermal stability and elemental diffusion behavior in liquid Sn.

Table 1. Chemical composition at the corresponding position in Fig. 2 – Fig. 5 by EDS analysis

Position	Ti, at%	Cu, at%	Sn, at%	Phases
Rods (Fig. 2)	64.9±4.5	35.1±3.1	0	Ti_2Cu
P1 (Fig. 3)	41.4	15.6	43.0	Ti_2Cu, Sn
P2 (Fig. 3)	23.6	76.2	0.2	$TiCu_2$
P3 (Fig. 3)	39.8	17.2	43.0	Ti_2Cu, Sn
P4 (Fig. 4)	47.3	8.3	44.4	Ti_6Sn_5, Ti_2Sn_3, $TiCu_2$
P5 (Fig. 4)	46.4	7.8	45.8	Ti_6Sn_5, Ti_2Sn_3, $TiCu_2$
P6 (Fig. 4)	45.9	4.3	49.8	Ti_6Sn_5, Ti_2Sn_3, $TiCu_2$
Rods (Fig. 5)	60.3±4.8	33.2±3.4	6.5±1.4	Ti_2Cu

3.2. Cu repartitioning via thermal diffusion in liquid Sn at 590 °C

Cross-sectional SEM morphology and elemental distribution profiles are shown in Fig. 3. After 5 s of thermal diffusion of $Ti_{30}Cu_{70}$ amorphous ribbons in liquid Sn at 590 °C, obvious contrast between the middle region and edge region in Fig. 3 a indicates the different distribution of Cu, Ti, and Sn and the Sn invasion. Overall elemental distribution in Fig. 3 b – e clearly demonstrates the relatively uniform distribution of Ti and lower-concentrated Cu in the edge region of original $Ti_{30}Cu_{70}$ amorphous ribbons. The chemical composition at the corresponding position marked as P1, P2 and P3 (Table 1) indicates the possible phase constituent of Ti_2Cu and Sn at P1 and P3 and Ti_2Cu at P2. The thickness of the undiffused layers was confirmed to be 17.05 μm. Moreover, the chemical composition in the regions with higher Ti content was confirmed to be 32.8 at%Cu, 0.5 at% Sn and 66.7 at%Ti, corresponding to Ti_2Cu IMCs. The residual in the middle region has a similar chemical composition to the as-spun $Ti_{30}Cu_{70}$ ribbons.

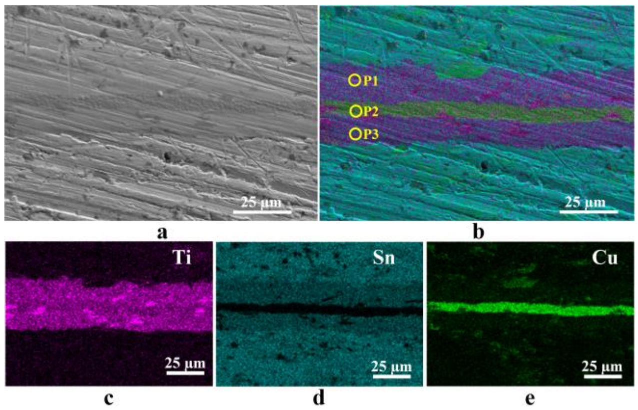

Fig. 3. Morphology and elemental distribution profiles in $Ti_{30}Cu_{70}$ amorphous ribbons after thermal diffusion of 5 s: a – cross-sectional SEM morphology; b – overall elemental mapping; c – Ti; d – Sn; e – Cu

With extention of thermal diffusion time to 30 s, there is still a thin residual $Ti_{30}Cu_{70}$ ribbon without serious Sn invasion. The thickness of the undiffused layers was confirmed to be 18.78 μm. Cross-sectional SEM morphology and elemental distribution profiles in Fig. 4. After 60 s of thermal diffusion of $Ti_{30}Cu_{70}$ amorphous ribbons in liquid Sn at 590 ℃, although there is concentration gradient of Cu element along the thickness direction, the concentration of Sn element is much higher than those in Fig. 3.

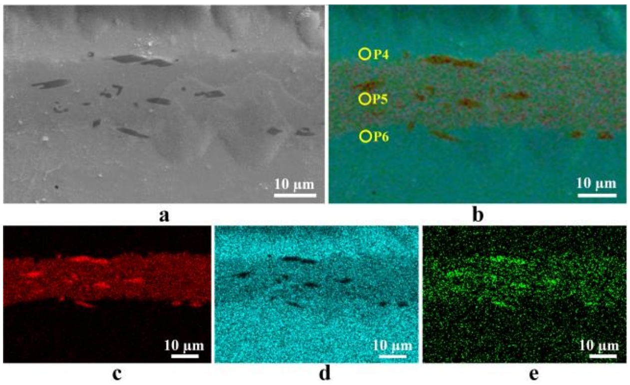

Fig. 4. Morphology and elemental distribution profiles in $Ti_{30}Cu_{70}$ amorphous ribbons after thermal diffusion of 60 s: a – cross-sectional SEM morphology; b – overall elemental mapping; c – Ti; d – Sn; e – Cu

Overall elemental distribution in Fig. 4 b – e clearly demonstrates the relatively uniform distribution of Ti and Sn. The chemical composition at corresponding position marked as P4, P5 and P6 indicates the possible phase constituent of Ti_6Sn_5, Ti_2Sn_3, $TiCu_2$ (as listed in Table 1). Some particles without Sn in Fig. 4 d were confirmed to be Ti_2Cu IMCs. On the basis of Fig. 3 d and 4d, Ti_2Cu IMCs remain unreacted in liquid Sn at 590 °C. The Sn diffused through the whole ribbon after 60 s. Cu elements are almost replaced by Sn elements via fast thermal diffusion. In order to confirm the phase constitute of thermal diffused $Ti_{30}Cu_{70}$ amorphous ribbons in liquid Sn at 590 °C for 60 s, XRD analysis was conducted on the samples after chemical etching for 18 h in 1 M HNO_3 solution to expose the residual IMCs. XRD pattern in Fig. 5 a indicates that the residual are composed of Ti_6Sn_5 (JCPDF Card No.:18-1390), Ti_2Sn_3 (JCPDF Card No.:52-0945), original Ti_2Cu IMCs and Ti (JCPDF Card No.:88-2321). The diffusion kinetics are built on the basis of the thickness changes in the residual layers in the middle region. The thickness of residual layers in Fig. 5 b is confirmed to 17.1 μm for 5 s, 18.8 μm for 30 s and 20.1 μm for 60 s. On the other hand, this change can be used to stand for the diffusion depth. The diffusion rate can be reflected by the slope and calculated to be 5.61×10^{-8} m s^{-1}. The surface morphology and elemental distribution are present in Fig. 5 c – f. Many bar-shaped IMCs have s similar outlines with those in Fig. 2 c, Fig. 3, and Fig. 4. These IMCs are confirmed to be Ti_2Cu in Table 1. The Sn invasion results to the formation of the new IMCs including Ti_6Sn_5 and Ti_2Sn_3. Cu elements are repartitioned through the thermal diffusion and formation of the new Sn-base IMCs.

In fact, when $Ti_{30}Cu_{70}$ ribbons were treated in liquid Sn at 420 °C for 1 h, there were no Sn-containing IMCs formed, and the newly-formed IMCs were confirmed to be Cu_6Sn_5. Ti_2Cu IMCs remain as thier original state, which is considered to be due to their high thermal stability. The liquidus temperature in Ti-Cu phase diagram is reported to be 960 °C for Ti_2Cu eutectic formation and 790 °C for Ti_2Cu solid eutectoid formation [12]. The Ti_2Sn_3 phases form through peritectic reaction of Ti_6Sn_5 and liquidus at 750 °C and eutectic reaction at 231.9 °C [13, 14].

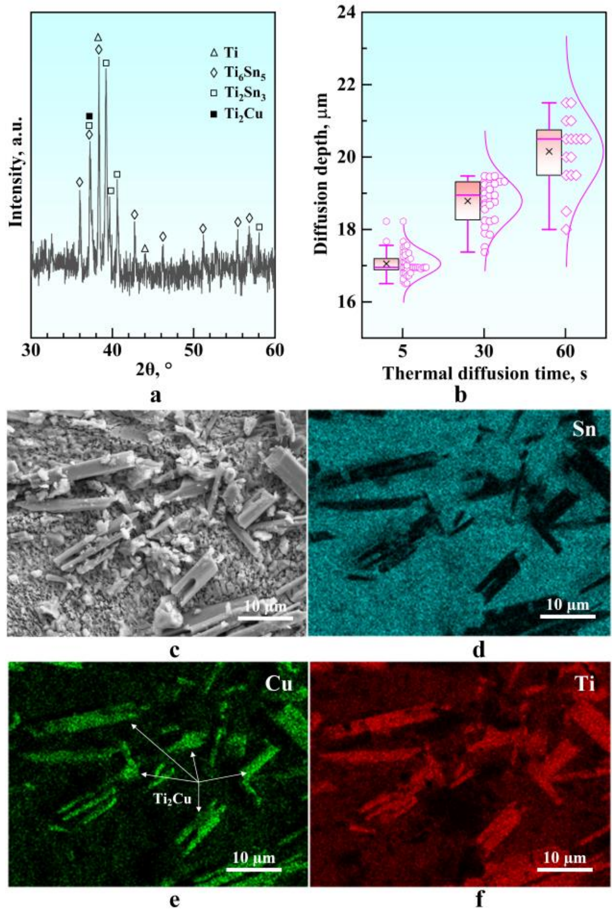

Fig. 5. Phase evolution and Sn/Cu partioning in $Ti_{30}Cu_{70}$ amorphous ribbons after thermal diffusion treatment of 60 s and following etching in 1 M HNO_3 for 18 h: a – XRD pattern of thermal diffusion treated $Ti_{30}Cu_{70}$ amorphous ribbons after etching in 1 M HNO_3 for 18 h; b – statistical analysis of the diffusion depth; c – top-view SEM morphology; d – Sn, e – Cu; f – Ti

However, the Cu-Sn phase diagram states that Cu_6Sn_5 phase can form via eutectic reaction at low temperature of 227 °C [4]. Secondly, the solubility of Cu and Ti in liquid Sn at 550 °C can be up to 40 at.% and nearly 10 at.%, respectively [4, 12, 13]. On basis of the difference in thermal stability and solubility of Cu_6Sn_5, Ti_2Cu, Ti_6Sn_5 and Ti_2Sn_3 [4, 12 – 15], the Cu_6Sn_5 compound with low reaction temperature acts as the intermediate reactant to help the replacement of Cu in $Ti_{30}Cu_{70}$ ribbons primarily. The thinning of the middle residual layers in Fig. 3 and Fig. 4 proves the fast interdiffusion of Cu and Sn during the thermal diffusion in liquid Sn. Moreover, Ti_2Cu IMCs remain unreactable due to their high reaction temperature of 790 °C as shown in Fig. 1 – Fig. 5. Therefore, it is proposed here that the elemental repartitioning can be achieved by an optimum combination of the solubility of various intermediate reactants and products, the right temperature zone where the solid-solid and liquid-solid reactions can be motivated by fast dissolution of specific IMCs, and the proper time duration for the thermal diffusion treatments. Many efforts have been extensively contributed to create heterogeneity in order to select the proper chemical composition suitable for better mechanical properties through high-throughout thermal diffusion coupling [16]. On the other hand, the surface enrichments of the active sites are supposed to be necessary in the field of catalytic fields. The establishments of the less-noble elements or phases in the surface region of target alloys help to create the potential precursors for chemical etching or specific functional surface [17]. If the temperature and treatment time can be regulated properly in thermal diffusions, the leaching out can be motivated to generate topologically complex nanoporous and nanocomposite structures in liquid metal dealloying [18]. The present research can contribute a new alloying method by using liquid-solid reactions through elemental repartitioning. The present methodology provides a possible way to fabricate the precursors with multilayers, where different intermetallic phases are distributed, too.

4. CONCLUSIONS

Thermal diffusion experiments of amorphous $Ti_{30}Cu_{70}$ ribbons with minor Ti_2Cu intermetallics were conducted in liquid Sn at 590 °C in order to trigger the fast interdiffusion of Sn and replace Cu elements by invaded Sn. The Cu elements are replaced partially by Sn elements gradually with the extension of treatment time, and most of Cu elements can be replaced by Sn at 60 s. Pre-existing Ti_2Cu intermetallic phases in amorphous $Ti_{30}Cu_{70}$ ribbons still remain as preformed due to their higher thermal stability. At last, both Ti_6Sn_5 and Ti_2Sn_3 intermetallic phases formed throughout $Ti_{30}Cu_{70}$ ribbons after thermal diffusion and replaced the intermediate Cu_6Sn_5 intermetallics with low reaction temperature and relatively large solubility of Cu in Sn. The repartitioning rate of Sn elements was calculated to be 5.61×10^{-8} m s^{-1} according to the change of the thickness of residual layers with high Cu concentration. The present methodology provides a possible way to fabricate the precursors with multilayers through different distributions of intermetallic phases and thermal alloying.

Acknowledgments

This work is financially supported by the National Science and Technology Major Project of the Ministry of Science and Technology of China and the National Natural Science Foundation of China under (Grant no. 52371157 & 51671106). This work is partially supported by Priority Academic Program Development of Jiangsu Higher Education Institution (PAPD).

REFERENCES

1. **Chaitanya, N.K., Yadav, B., Bhattacharjee, P.P., Vaidya, M.** Effect of Ultrafine Microstructure on Interdiffusion-driven Phase Transformations in Ni-Sn Sandwich Diffusion Couples *Materials Today Communication* 35 2023: pp. 105843. https://doi.org/ 10.1016/j.mtcomm.2023.105843
2. **Li, J.F., Agyakwa, P.A., Johnson, C.M.** Interfacial Reaction in Cu/Sn/Cu System during the Transient Liquid Phase Soldering Process *Acta Materialia* 59 (3) 2011: pp. 1198 – 1211. https://doi.org/10.1016/j.actamat.2010.10.053
3. **Tao, C.Y., Tu, M.S., Huang, H., Chang, H., Dan, Z.H.,** Tri-modal Hierarchical Nanoporous Copper as Hydrogen Evolution Reaction Catalysts with Low Tafel Slopes via Stepwise Fabrication of Surface Alloying in Molten Tin and Electrochemical Dealloying of Copper Foams *Journal of Alloys and Compounds* 1037 2025: pp. 182391. https://doi.org/10.1016/j.jallcom.2025.182391
4. **Saunders, N., Miodownik, A.P.** The Cu-Sn (copper-tin) System *Bulletin of Alloy Phase Diagrams* 11 (3) 1990: pp. 278 – 287. https://doi.org/10.1007/BF03029299.
5. **Wang, J.T., Lv, Z.W., Zhang, L.B., Duan, F.C., Wang, J.Q., Li, F.Q., Chen, H.T., Li, M.Y.** Nucleation and Growth of Cu_6Sn_5 during the Aging Process of Cu/Sn Interface in Electronic Packaging-by In-situ TEM *Acta Materialia* 264 2024: pp. 119581. https://doi.org/10.1016/j.actamat.2023.119581
6. **Yuan, Y., Guan, Y.Y., Li, D.J., Moelans, N.** Investigation of Diffusion Behavior in Cu-Sn Solid State Diffusion Couples *Journal of Alloys and Compounds* 661 2016: pp. 282 – 293. https://doi.org/10.1016/j.jallcom.2015.11.214
7. **Yang, G.L., Li, X.Y., Han, X., Li, S.S.** Effect of Isothermal Storage on the Microstructure and Grain Orientation of Cu/Cu_3Sn/Cu Solder Joint *Soldering & Surface Mount Technology* 35 (1) 2023: pp. 44 – 50. https://doi.org/10.1108/SSMT-04-2022-0034
8. **Inoue, A.** Stabilization of Metallic Supercooled Liquid and Bulk Amorphous Alloys *Acta Materialia* 48 2000: pp. 279 – 306. https://doi.org/10.1016/S1359-6454(99)00300-6
9. **Dan, Z.H., Qin, F.X., Sugawara, Y., Muto, I., Hara, N.** Fabrication of Nanoporous Copper by Dealloying Amorphous Binary Ti-Cu Alloys in Hydrofluoric Acid Solutions *Intermetallics* 29 2012: pp. 14 – 20. https://doi.org/10.1016/j.intermet.2012.04.016
10. **Xu, Z.X., Erinomo, A.M., Dan, Z.H., Qin, F.X., Chang, H.** Flexible SERS Substrates with Gradient Porous Cu Structure Dealloying from the Thermal Diffusion Couples of Al/Cu Stacking Foils *Chemical Engineering Journal* 490 2024: pp. 151871. https://doi.org/10.1016/j. cej.2024.151871
11. **Dan, Z.H., Zhang, Y., Takeuchi, A., Hara, N., Qin, F.X., Makino, A., Chang, H.** Effect of Substitution of Cu by Au and Ag on Nanocrystallization Behavior of $Fe_{83.3}Si_4B_8P_4Cu_{0.7}$ Soft Magnetic Alloy *Journal of Alloys and Compounds* 683 2016: pp. 263 – 270. http://doi.org/10.1016/j.jallcom.2016.05.027
12. **Murray, J.L.** The Cu-Ti (Copper-Titanium) System *Bulletin of Alloy Phase Diagrams* 4 (1) 1983: pp. 81 – 95. https://doi.org/10.1007/BF02880329
13. **Kuper, C., Peng, W.Q., Alexander, P., Goesmann, F., Schmid-Fetzer, R.** Phase Formation and Reaction Kinetics in the System Ti-Sn *International Journal of Materials Research* 89 (12) 1998: pp. 855 – 862. https://doi.org/10.3139/ijmr-1998-0165
14. **Zhou, G.J., Zhou, Y., Luo, Y.** Phase Equilibria of the Cu-Sn-Ti Ternary System at 823K *AIP Advances* 7 (2) 2017: pp. 025118. http://dx.doi.org/10.1063/1.4975220
15. **Yin, F.C., Tedenac, J.C., Gascoin, F.** Thermodynamic Modelling of the Ti-Sn System and Calculation of the Co-Ti-Sn System *Calphad* 31 (3) 2007: pp. 370 – 379. https://doi.org/10.1016/j.calphad.2007.01.003
16. **Liu, K., Yu, H.C., Li, X., Wu, S.J.** Study on Diffusion Characteristics of Al-Cu Systems and Mechanical Properties

of Intermetallics *Journal of Alloys and Compounds* 874 2021: pp. 159831. https://doi.org/10.1016/j.jallcom.2021.159831

17. **Liu, J., Jia, J.H., Chen, L.B., Meng, H., Ran, Q., Shi, H., Han, G.F., Wang, T.H., Wen, Z., Lang, X.Y., Jiang, Q.** Gradient Nanoporous Copper–Zinc Alloy Regulating Dendrite-Free Zinc Electrodeposition for High-Performance Aqueous Zinc-Ion Batteries *Nano Letters* 25 (11) 2025: pp. 4298 – 4306. https://doi.org/10.1021/acs.nanolett.4c06181
18. **Geslin, P.A., McCue, I., Gaskey, B., Erlebacher, J., Karma, A.** Topology-generating Interfacial Pattern Formation during Liquid Metal Dealloying *Nature Communications* 6 2015: pp. 8887. https://doi.org/10.1038/ncomms9887